FINITE ELEMENT SIMULATION OF RESIDUAL STRESSES AND DISTORTIONS IN SELECTIVE LASER MELTING

M. KAESS*, M. WERZ** and S. WEIHE**

*Institute for Materials Testing, Materials Science and Strength of Materials (IMWF), University of Stuttgart, Germany
**Materials Testing Institute (MPA), University of Stuttgart, Germany

DOI 10.3217/978-3-85125-615-4-16

ABSTRACT

With additive manufacturing, the production of individual lightweight structures and complex parts with integrated functions can be realized. In selective laser melting (SLM), a highly concentrated and fast moving laser spot is used to melt the powder layers which leads to high temperature gradients during the manufacturing process. This causes thermal residual stresses and distortions which can affect the intended use of additive manufactured parts. If cracks and distortions develop during the manufacturing process, a collision of the powder coater with the manufactured part can lead to a process abortion. A simulation predicting residual stresses and distortions can be used to consider these problems before manufacturing and therefore avoid scrap parts. Parameter configurations could be developed systematically to reach specific component properties. A common approach for simulating these effects in welding is the thermomechanical finite element simulation. Using this approach with a high spatial and temporal resolution, which is necessary to accurately represent the heat source, only small additive manufactured parts can be simulated with a reasonable computational effort. In order to allow numerical simulations of parts with larger dimensions, it is necessary to use appropriate simplifications and simulation strategies. One possible simplification presented in literature is to expose a whole layer to a heat source simultaneously instead of considering the whole scan path. To evaluate the effect of this simplification, the SLM-manufacturing of cuboids is simulated with different temporal resolution. Moreover, the effects of a base plate cutting and of different scanning strategies on residual stresses and distortions are examined numerically.

Keywords: selective laser melting, simulation, temperature fields, residual stresses, distortions

INTRODUCTION

Due to its unique advantages, compared to conventional manufacturing methods, additive manufacturing has become rather popular. Additive manufacturing methods allow the production of individually produced complex components which also allows the construction of lightweight structures and components with integrated features. Compared to traditional manufacturing processes, such as forging or drilling, part or process specific tools are not needed in additive manufacturing. This provides geometry and designing choices which, in return, allows for complex, innovative and bionically optimized

structures. Since only the CAD data is needed to manufacture these components, smaller quantities can be produced rather quickly.

During selective laser melting, a powdered base material is applied in layers and melted locally by means of a laser source. During the following cool down, the new material solidifies and forms solid connections with the already existing layers. This process can be compared to multilayer welding and shape welding. Only the area where the part is created is melted in each layer. The other surrounding areas stay in powder form. This powder is removed once the process is completed.

Due to the highly focused and rapidly moving heat source, there are thermal expansions and contractions during SLM [1]. If these thermal expansions or contractions are in any way obstructed during the heating or cooling of the components, local plastifications can occur due to an exceeded yield strength and thermal residual stresses could be the result [1], [2], [3]. The extent of the thermal expansions depends on locally varying heat gradients. During the SLM process, the thermal expansion, caused by the heating of the upper layers of the components, is blocked by the solidified layers underneath or the base plate respectively. Due to the higher temperatures, the material in the upper areas has a lower yield strength which tends to lead to increased yielding [4]. Residual stresses can result in cracks or can have negative effects on the tolerable loads during operation [1], [5]. Furthermore, distortions of the components can be caused by residual stresses [1], which, in return, can lead to unwanted deviations of the shape and even to the collision of the component with the mechanism that applies the powder during production. A process simulation to predict residual stresses and deviations could help to factor in these influences before the start of production. With a good simulation, parameter configurations could be developed, tested and used to achieve specific component characteristics. The different length scales of process and part, however, still pose a challenge for FE-simulations of SLM manufacturing. Currently, the dimension of additively manufactured parts can reach several centimeters or even decimeters and, on the other hand, the laser spot diameter and layer thickness are in the order of about 100 micrometers. In order to display the exact movement of the laser, a high-resolution simulation of the processing time and the working area is inevitable. Such a simulation, however, requires an immense computing effort, especially when done for larger parts. Adequate simplifications and calculation strategies need to be developed to reduce these computing efforts of numerical simulations for real life components.

STATE OF THE ART

Numerous approaches for numerical simulations of temperature fields [6], [7], [8], [9] and residual stresses as well as deformations [10], [11], [12], [13], [14] during selective beam welding processes are described by many authors. Especially thermomechanically coupled finite element calculations are often used to determine residual stresses and deformations.

Goldak [15], [16] developed a heat source with Gaussian distribution for the fusion welding process to describe the heat input in great detail. Several different forms of heat sources for the numerical simulation of the laser beam during the SLM process for additive manufacturing have been described in literature. Examples for such forms are circular surface heat sources [8], [9], [17] and circular volumetric heat sources [18], [19] which use

Gaussian intensity distribution. Furthermore, some authors describe the usage of heat sources with evenly distributed intensities [7], [20].

However, a high temporal and spatial resolution, which is necessary to precisely represent the laser spot diameter, laser movement as well as the layer thickness of a real life component, can cause very high computational costs. This is why residual stresses and temperature fields are often only calculated for smaller components. Some authors discuss methods that would allow to compute residual stresses and deformations for bigger parts as well: Keller et al. [11], for instance, use a multiscale approach with three stages to cope with the different length scales in selective laser melting to calculate residual stresses and distortions. In order to do so, the parameters of a Goldak heat source are calibrated in a microscopic model. What follows is a thermomechanical calculation using a simplified equivalent heat source in a meso-model to calculate a strain field for each layer considering the laser path. These inherent strains are finally used as input for a mechanical multi-layer calculation (macro-model), which requires less computing resources and is therefore more suitable for simulations of whole components [11].

Li et al. [13] also use a multi-scale approach with three stages. The microscale model is used to calculate the temperature field of the melt pool considering a heat source with Gaussian distribution on one single scan line. In the larger mesoscale model, the heating of a layer is simulated by using a simplified heat source which is applied for an exposure time determined in the microscale model. With the macroscale model, the layer-by-layer build process is simulated in a thermomechanically coupled analysis using the thermal input calculated in the mesoscale layer model. First, the transient temperature field of the whole build process is calculated in a thermal simulation and in a following mechanical simulation this thermal load is used to calculate stresses and strains for the whole model [13]. Neugebauer et al. [12] describe another way of simplification: To allow the usage of larger elements, multiple layers of the SLM process are combined in a macroscopic model. Furthermore, a highly detailed resolution of laser path is omitted in this approach. Instead, the layers are fully or partially heated simultaneously by one heat source. In the second case, the influence of the laser's path can, at least partially, be taken into account. The total amount of heat energy applied in this model is identical to the energy that would be applied by a high-resolution heat source. Due to the fact that in the real process the laser needs more time to run the scanning path, extra time is added in the simulation without a heat source being active. In this way, cooling processes, which occur during the heating in a real manufacturing process, can be taken into account [12].

Some authors use a method of local mesh refinement to allow for a detailed resolution of the heat source while at the same time granting a reasonable computing effort for large components [9], [10], [14], [21]. With this approach, the different length scales of SLM can be dealt with in one model. If a dynamic mesh refinement method is used, only the area immediately around the heat source is refined, the outer areas are less detailed. Due to boundary conditions or interpolations, information between the lesser and the more refined areas still need to be exchanged [21]. This is why in most commercial FE-codes the method of local mesh refinement is not realizable for AM processes [10]. This restricts the usage of dynamic mesh refinement methods to the case when no specific software is available.

Process simulations allow to manufacture components that are optimized for residual stresses. Moreover, a deeper understanding of the development of residual stresses is necessary to realize process simulations with acceptable computing efforts for large

components. Only a thorough understanding can lead to the development of adequate simplifications and computing methods, which, in return, would allow calculations for larger parts.

In our earlier works [22], [23], [24], it was investigated how deformations, residual stresses and temperature fields during the SLM process could be predicted by means of numerical simulations. Since the thermomechanically coupled finite-element-method for simulating the processes during welding has proven to be adequate, the same method was used to simulate the manufacturing of cuboids using SLM. In order to conduct numerical simulations with an agreeable amount of computing, simplifications had to be made. Therefore, the influence of the spacial and temporal discretization on the computing time and the preciseness of the simulation were investigated. A possible way to simplify the simulation is to combine the sections of the laser movement into larger intervals. Previous studies [22], [23], [24] show that this method is a possible way to simplify the process while losing only a small amount of detail. If the scanning strategy is simplified too much, however, not all aspects of the transient influences can be captured. The studies regarding the influence of element size, temperature gradients, residual stresses and deformations show consistent results as long as the size of the used elements does not exceed the diameter of the laser source or the thickness of the layers.

MODEL DESCRIPTION

Numerical studies have been performed to develop an understanding of influences of the base plate cutting and the scanning strategy on residual stresses and distortions in SLM. Moreover, the effects of a simplification method have been examined.

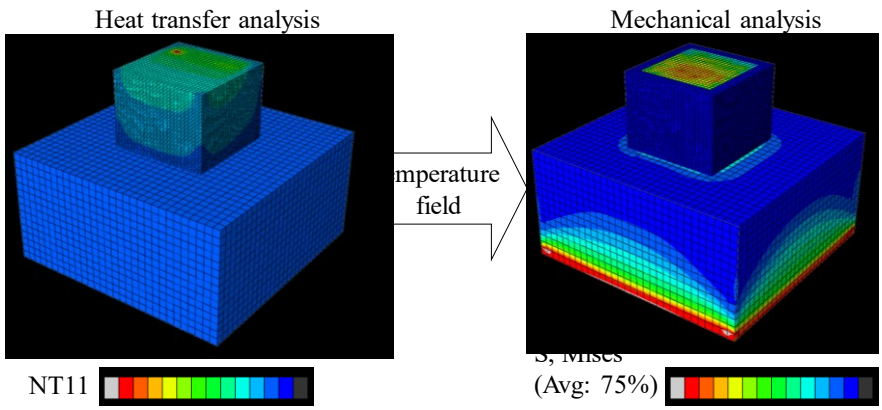

Fig. 1 Sequentially coupled thermomechanical simulation method shown schematically

In the presented studies, a sequentially coupled thermomechanical simulation approach is used in the finite element program Abaqus. Fig. 1 shows schematically the two models used for the implicit heat transfer analysis first, and the following implicit mechanical analysis second. In the heat transfer analysis, thermal boundary conditions and a heat source model to simulate the laser beam are applied. The result file from the heat transfer analysis is read into the sequentially coupled mechanical analysis to consider temperature dependent

material properties and to calculate thermal expansions and constrictions from temperature gradients. The mechanical analysis is being used to calculate stresses, strains and displacements considering mechanical boundary conditions.

In the studies, the model of a cube with 3 mm edge length, shown in Fig. 2, has been created. A tie contact is used in the model to simulate the connection to the base plate on which the cube is directly built. The element size in the cube is 0.15 x 0.15 x 0.05 mm³ and in the built plate it is 0.3 x 0.3 x 0.3 mm³. The element height of 0.05 mm represents the simulated powder layer thickness. Heat dependent material properties of the aluminum alloy AlSi10Mg in solid state are assigned to the base plate and the cube. Additionally, a material definition of AlSi10Mg with reduced thermal conductivity and reduced mechanical strength properties is used for the surrounding powder ring, which is modeled to account for the influence of the powder bed. The used material properties are shown in Table 1. The temperature dependent material properties are interpolated linearly in the given range and kept constant for lower and higher values.

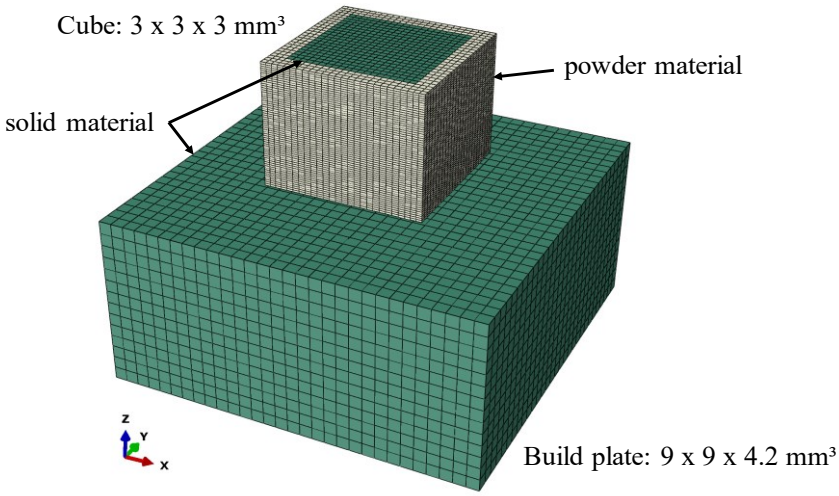

Fig. 2 Finite element model of a cube with build plate and different material assignments

The layer-by-layer build process is simulated by successively activating the elements of the cube. In the model, the final geometry of the cube is defined, but elements of a layer remain inactive until the coating of this layer is simulated. Inactive elements are not considered in the calculation. The new plug-in feature “AM Modeler” of Abaqus 2017 is used to control this element activation.

Table 1 Temperature-dependent material properties for powder and solid (derived from [25], [26])

temperature	20 °C		600 °C
heat conduction solid material	110 W/(m*K)		150 W/(m*K)
heat conduction powder material	1,1 W/(m*K)		1,5 W/(m*K)
heat capacity	900 J/(kg*K)		1200 J/(kg*K)
heat expansion	$21*10^{-6}$ 1/K		$26*10^{-6}$ 1/K
temperature	20 °C	500 °C	580 °C
yield strength powder material	1 MPa	1 MPa	1 MPa
Young's modulus powder material	10 GPa	10 GPa	10 GPa
yield strength solid material	250 MPa	20 MPa	1 MPa
Young's modulus solid material	72 GPa	10 GPa	10 GPa

With this Abaqus feature, it is also possible to define a heat source and the related scanning strategy for simulating the thermal impact of the laser beam. In this way, a hemi-spherical volumetric heat source with Gaussian intensity distribution was implemented in the model. A scanning speed of 1000 mm/s, a diameter of 0.2 mm and a power of 300 W were used for the heat source model.

At the top surface of the cube, convection and radiation to the build chamber are modelled in the heat transfer analysis. Furthermore, heat transfer to the surrounding powder bed is modelled at the lateral surfaces of the cube and heat transfer to the continuing built plate is modelled at the bottom. In the mechanical analysis, an encastre boundary condition is used for the bottom surface of the build plate to simulate a fixation in the SLM-machine.

For all simulations, a preheating of powder, build plate and build chamber to 50 °C is applied. After the build process of 60 layers with alternating element activation and layer heating, a cooling period follows in which the whole model is cooled down to room temperature (20 °C). Finally, the cutting process is simulated according to [27] by successively deleting the top element layer of the base plate, as shown in Fig. 3.

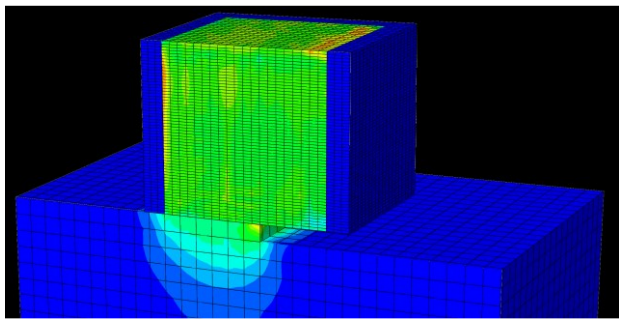

Fig. 3 Cutting from the build plate by deleting elements

With the model described above, studies of different scanning strategies were performed. These five examined scanning strategies are shown in Fig. 4. The scanning pattern remains unchanged for all layers in (a), (c) and (d) and alternates for (b) and (e). For scanning strategies a) to c), the scanning path starts in the upper left corner and ends in the lower right corner. The order of the islands is numbered for scanning strategy e).

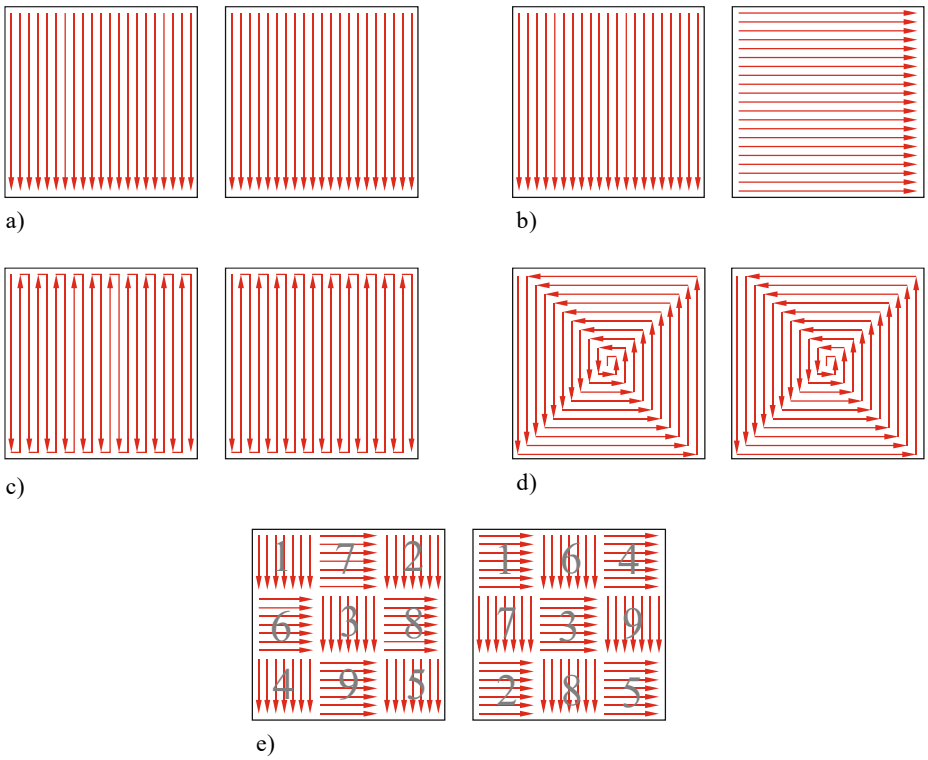

Fig. 4 scanning strategies - left and right figure represent alternating layers:
(a) linear scanning; (b) across scanning; (c) meander scanning; (d) screw scanning; (e) island scanning

RESULTS

Stresses and deformations are being analyzed along different paths, which are schematically shown in the cubic model in Fig. 5. Before build plate cutting, the cube is connected to the substrate on the x, y plane. Stresses are always taken along path 1 which is located in z-direction at the center of the cube. Distortions are calculated as a difference of displacements on two paths located on opposite surfaces. Path 2a and 2b are used to calculate the shrinkage or expansion in z-direction and along path 3a and 3b, the deformation in x-direction is analyzed.

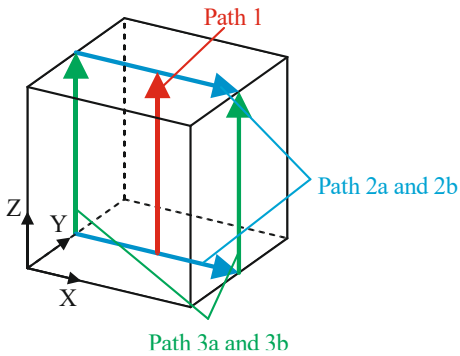

Fig. 5 Paths in the cubic model to analyze stresses and deformations

Fig. 6 and Fig. 7 show how stresses and distortions change in the model due to a base plate cutting. These simulations have been conducted with a linear scanning strategy and a time increment of 0.001 s. Mercelis et al. [4] determined that parts which are removed from the base plate basically show tensile stresses in the upper region, compressive stresses in the center and tensile stresses in the lower areas. The occurrence of high tensile stresses in the top layers and compressive stresses in the center of parts is confirmed by [1]. The stresses in x-direction illustrated in Fig. 6 show a good qualitative accordance to the distribution described in [1] and [4].

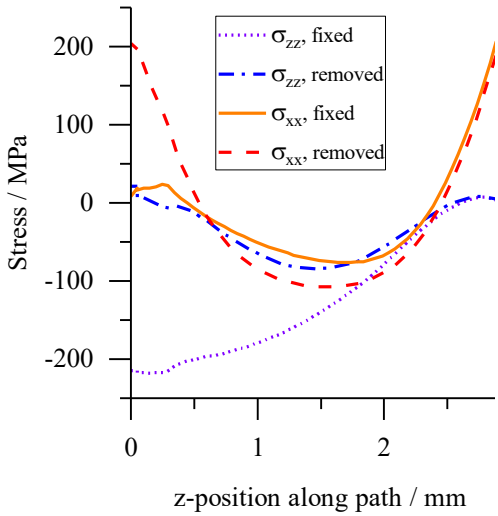

Fig. 6 Influence of base plate cutting on stresses along path 1 – linear scanning strategy

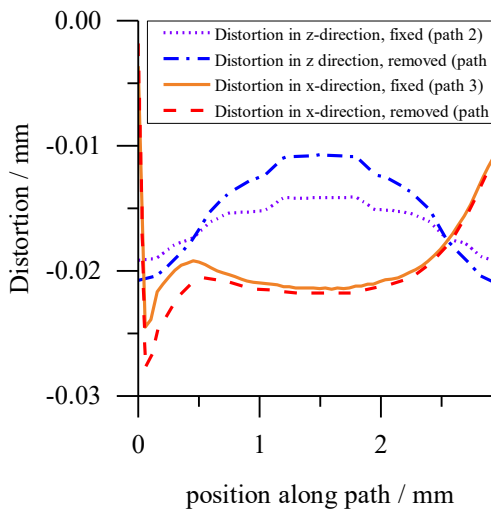

Fig. 7 Influence of base plate cutting on distortions along paths 2 and 3 – linear scanning strategy

Fig. 6 shows high compressive stresses in z-direction along path 1 in the bottom area of the cube before cutting from the base plate. A relaxation of these stresses occurs when the base plate is removed. On the other hand, high tensile stresses emerge in x-direction after base plate cutting. In Fig. 7, the geometrical deviation from the ideal shape is shown. This means that an expansion in z-direction and a shrinkage in x-direction occurs due to the base plate cutting. In summary, it could be shown that significant changes of stresses occur at

the bottom of the cube whereas the upper area remains almost unchanged when the base plate is removed. These variations of the stress field cause shrinkage and expansion of the cube.

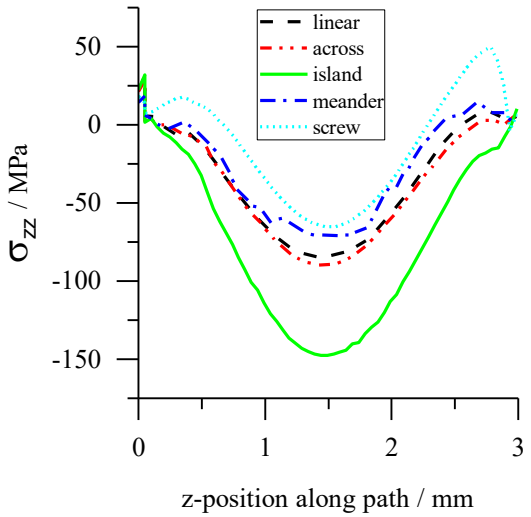

Fig. 8 σ_{zz} along path 1 for different scanning strategies – used time increment: 0.001 s

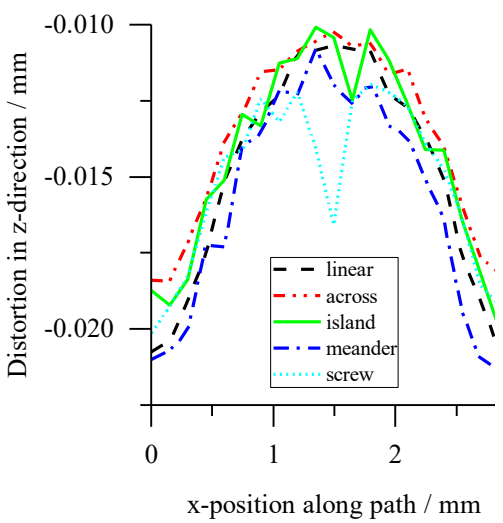

Fig. 9 distortion in z-direction along paths 2 – used time increment: 0.001 s

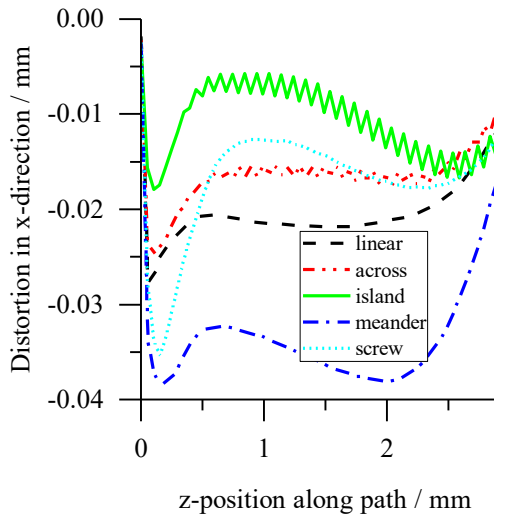

Fig. 10 distortion in x-direction along paths 3– used time increment: 0.001 s

The influence of different scanning strategies on residual stresses after base plate cutting is shown in Fig. 8. All calculated stress curves have a similar shape but show different minimum and maximum values. The highest compressive stresses in z-direction occur in the center of the cube for an island scanning strategy.

Fig. 9 and Fig. 10 show the geometrical deviations for different scanning strategies after base plate cutting. Only small differences are calculated for the deformation in z-direction,

but significant variations occur for the deformation in x-direction. The largest shrinkage in x-direction has been calculated for a meander scanning strategy and the smallest deviation is shown for an island scanning pattern. This means that the simulation method can be used to capture effects of different scanning strategies. A validation of the numerical results has to be done in a future study to allow a quantitative comparison.

In the following, an examination of different temporal discretizations is presented. Fig. 11 shows the stress in z-direction along path 1 for a linear scanning strategy. Only with a small time increment, the scanning strategy can be considered in detail. For larger time increments, the heat flux is averaged over larger segments of the scanning path which are passed by the fast moving laser beam. Using a time increment of 0.1 s means that one whole layer is heated at the same time. In Fig. 11 it can be seen that wide variations of the calculated residual stresses occur. Convergence of the results can be seen for a time increment equal or smaller than 0.0005 s. Averaging the heat fluxes over a long period of time means that the spot heating with high intensity cannot be considered in the calculation and the maximum temperatures that are reached decrease. This has already been shown in [22], [23] and [24].

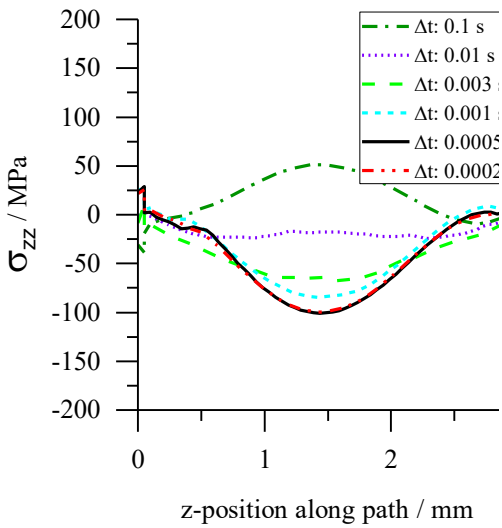

Fig. 11 σzz along path 1 for different temporal discretizations – linear scanning strategy

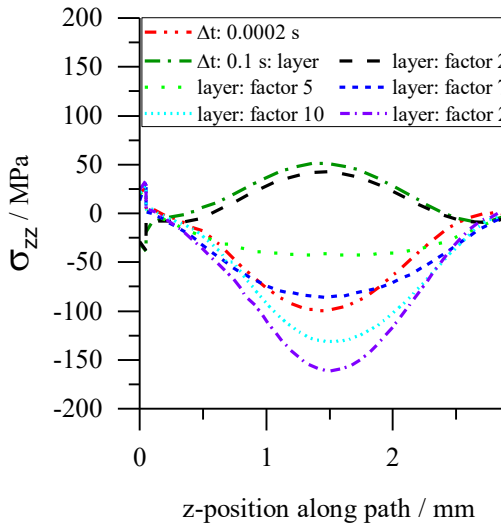

Fig. 12 σ_{zz} along path 1 for different temporal discretizations and layer-by-layer heating – linear scanning strategy

A layer-by-layer heating with higher intensity for a respectively shorter period of time was tested to compensate this effect of averaged heat fluxes and decreasing temperatures. For this purpose, the intensity of the layer heat source was increased by a factor between 2 and 20 and the exposure time was reduced by the same factor. As a result, the energy input per unit length and the total energy input per layer were kept constant. In

Fig. 12 Fig. 12, it is shown that this technique allows to adjust the calculated residual stresses to the shape calculated with a high temporal resolution (0.0002 s). However, if the factor is too high, the calculated residual stresses exceed the curve with high resolution (0.0002 s).

In Fig. 12 the curve with a factor of 7 shows the best results for the stresses in z-direction. For other magnitudes, like σ_{xx} or deformations, the factor also shows an effect and can be used to match the curves. However, the ideal factor varies for the different magnitudes. For example, a factor of 15 or even 30 is best to fit the stress or deformation in x-direction in this model. This means that a layer-by-layer heating could be an appropriate method of simplification to reduce computational effort if the intensity of the heat source is calibrated well. In future studies, different calibration methods, based on the maximum temperatures reached in the process or the energy input per unit length, will be examined. However, the effect of different scanning strategies, as shown in Fig. 8 and Fig. 10, cannot be considered by a layer heat source. This effect could perhaps be dealt with if a calibration of the layer heat source is conducted with a detailed model of one or a few layers.

CONCLUSION

It could be shown that a base plate cutting and different scanning strategies can be considered in a thermomechanical finite element simulation of a selective laser melting process. A high temporal resolution is necessary to model the effect of different scanning strategies. On the other hand, it was shown that a layer-by-layer heating could be an appropriate method to reduce computational costs. Simplifications are important to make the thermomechanical finite element method feasible for simulating the SLM-production of large components. In future studies, it is planned to additively manufacture cubes and other geometries and experimentally examine these parts on residual stresses and distortions. These experimental studies are necessary to validate and develop the models and the proposed simplification strategies.

REFERENCES

[1] Y. LIU, Y. YANG, and D. WANG, ‘A study on the residual stress during selective laser melting (SLM) of metallic powder’, *Int J Adv Manuf Technol*, vol. 87, no. 1-4, pp. 647–656, 2016.

[2] E. ROOS, K. MAILE, and M. SEIDENFUß, *Werkstoffkunde für Ingenieure,* 6th ed. Berlin: Springer-Vieweg, 2017.

[3] D. BUCHBINDER, G. SCHILLING, W. MEINERS, N. PIRCH, and K. WISSENBACH, ‘Untersuchung zur Reduzierung des Verzugs durch Vorwärmung bei der Herstellung von Aluminiumbauteilen mittels SLM’, *RTejournal*, 2011.

[4] P. MERCELIS and J. KRUTH, ‘Residual stresses in selective laser sintering and selective laser melting’, *Rapid Prototyping Journal*, vol. 12, no. 5, pp. 254–265, 2006.

[5] C. CASAVOLA, S. L. CAMPANELLI, and C. PAPPALETTERE, ‘Preliminary investigation on distribution of residual stress generated by the selective laser melting process’, *The Journal of Strain Analysis for Engineering Design*, vol. 44, no. 1, pp. 93–104, 2008.

[6] S. KOLOSSOV, E. BOILLAT, R. GLARDON, P. FISCHER, and M. LOCHER, ‘3D FE simulation for temperature evolution in the selective laser sintering process’, *International Journal of Machine Tools and Manufacture*, vol. 44, no. 2-3, pp. 117–123, 2004.

[7] N. CONTUZZI, S. L. CAMPANELLI, and A. D. LUDOVICO, ‘3D Finite Element Analysis in the selective laser melting process’, *Int. j. simul. model.*, vol. 10, no. 3, pp. 113–121, 2011.

[8] I. A. ROBERTS, C. J. WANG, R. ESTERLEIN, M. STANFORD, and D. J. MYNORS, 'A three-dimensional finite element analysis of the temperature field during laser melting of metal powders in additive layer manufacturing', *International Journal of Machine Tools and Manufacture*, vol. 49, no. 12-13, pp. 916–923, 2009.

[9] D. PITASSI *et al.,* 'Finite Element Thermal Analysis of Metal Parts Additively Manufactured via Selective Laser Melting' in *Finite Element Method - Simulation, Numerical Analysis and Solution Techniques*, R. Păcurar, Ed.: InTech, 2018.

[10] A. BAUEREIß, E. PARTELI, D. RIEDLBAUER, and M. STINGL, 'Numerische Simulation pulver- und strahlbasierter additiver Fertigungsprozesse', *in Dietmar Drummer*, pp. 117–130, 2012.

[11] N. KELLER and V. PLOSHIKHIN, 'New method for fast predictions of residual stress and distortion of AM parts'. Austin, Texas, 2014.

[12] F. NEUGEBAUER, N. KELLER, V. PLOSHIKHIN, F. FEUERHAHN, and H. KÖHLER, 'Multi Scale FEM Simulation for Distortion Calculation in Additive Manufacturing of Hardening Stainless Steel'. Bremen, 2014.

[13] C. LI, J. F. LIU, X. Y. FANG, and Y. B. GUO, 'Efficient predictive model of part distortion and residual stress in selective laser melting', *Additive Manufacturing*, vol. 17, pp. 157–168, 2017.

[14] E. R. DENLINGER, M. GOUGE, J. IRWIN, and P. MICHALERIS, 'Thermomechanical model development and in situ experimental validation of the Laser Powder-Bed Fusion process', *Additive Manufacturing*, vol. 16, pp. 73–80, 2017.

[15] J. GOLDAK, A. CHAKRAVARTI, and M. BIBBY, 'A new finite element model for welding heat sources', *Metallurgical Transactions*, no. 15B, pp. 299–305, 1984.

[16] J. GOLDAK and M. AKHLAGHI, *Computational welding mechanics*.

[17] K. ZENG, D. PAL, N. PATIL, and B. STUCKER, 'A new Dynamic Mesh Method Applied to the Simulation of Selective Laser Melting'. Austin, Texas, 2013.

[18] T. TÖPPEL, B. MÜLLER, K. P. HOEREN, and G. WITT, 'Eigenspannungen und Verzug bei der additiven Fertigung', *Schweißen und Schneiden 68*, no. 4, pp. 176–186, 2016.

[19] A. HUSSEIN, L. HAO, C. YAN, and R. EVERSON, 'Finite element simulation of the temperature and stress fields in single layers built without-support in selective laser melting', *Materials & Design (1980-2015)*, vol. 52, pp. 638–647, 2013.

[20] A. FOROOZMEHR, M. BADROSSAMAY, E. FOROOZMEHR, and S. GOLABI, 'Finite Element Simulation of Selective Laser Melting process considering Optical Penetration Depth of laser in powder bed', *Materials & Design*, vol. 89, pp. 255–263, 2016.

[21] N. PATIL, D. PAL, and B. STUCKER, 'A New Finite Element Solver using Numerical Eigen Modes for Fast Simulation of Additive Manufacturing Processes'.

[22] M. KÄß, 'Entwicklung einer Simulationsmethode zur Vorhersage der Eigenspannungen beim selektiven Laserschmelzen (SLM)', Master's Thesis, Institute für Materials Testing, Materials Science and Strength of Materials (IMWF), University of Stuttgart, 2017.

[23] M. KÄß, M. WERZ, and S. WEIHE, 'Vergleich verschiedener Ansätze zur Simulation der Temperaturfelder und Eigenspannungen beim selektiven Laserschmelzen', *2. Tagung des DVM Arbeitskreises - Additiv gefertigte Bauteile und Strukturen*, pp. 99–112, 2017.

[24] M. KÄß, M. WERZ, and S. WEIHE, 'Parametrische Untersuchung der Diskretisierung für die numerische Simulation von Temperaturfeldern, Eigenspannungen und Verzügen beim selektiven Laserschmelzen', *DGM Fachtagung Werkstoffe und Additive Fertigung*, 2018.

[25] EOS GmbH, 'Materialdatenblatt EOS Aluminium AlSi10Mg', Krailing/München, 2014.

[26] Renishaw plc, 'AlSi10Mg-0403 Pulver für die generative Fertigung', Pliezhausen, 2015.

[27] T. BARETH, 'Entwicklung eines Modells zur Simulation von Eigenspannungen und Verzügen beim selektiven Laserschmelzen', Student Research Project, Institute für Materials Testing, Materials Science and Strength of Materials (IMWF), University of Stuttgart, 2018.